13

The Maskless litographer of direct drawing. Design, structure and application

© A.I. Artyukhov, S.S. Morozov, D.V. Petrova, N.I. Chkhalo, R.A. Shaposhnikov

Institute of Physics of Microstructures, Russian Academy of Sciences,
607680 Nizhny Novgorod, Russia
e-mail: artuhov@ipmras.ru

Received May 13, 2024
Revised May 13, 2024
Accepted May 13, 2024

The article presents the results of the development the maskless litographer of direct drawing, which allows to form the „windows“ in the photoresist layer by the beam with a diameter of 10 μm, with a moving accuracy of up to 2.5 μm and edge evenness of up to 10 μm. The technic structure of the lithographer and the operating principle of the main components of the device are described. Special software was developed to the lithographer control. The developed device was successfully tested for the range of technical goals, includes the making the multilayer multistrip X-ray mirrors.

Keywords:: the maskless litographer of direct drawing, the optic system, the multilayer multistrip X-ray mirrors.

DOI: 10.61011/TP.2024.08.59007.165-24

Introduction

The task of creating multi-strip mirrors emerged as part of the work on the creation of diagnostic elements for X-ray sources based on inverse Compton scattering [1], as well as for the creation of a two-mirror monochromator of SKIF synchrotron [2]. A multi-strip mirror is a set of multilayer X-ray mirrors located on a single substrate and differing in the period of the multilayer structure. This type of coatings can be formed on a single substrate by gluing cut strips with multilayer reflective coatings onto a single base, as proposed in Ref. [3]. However, this approach results in significant mismatch of local angles of incidence of radiation due to deformation of individual elements in the process of adhesive drying, different thicknesses of individual elements and adhesive layer.

Sometimes it is not possible to create such structures with different periods of multilayer coatings by sputtering of gradient coatings [4] because of the very different values of the period gradient along and across the mirror [5].

Sputtering through a metal mask located in close proximity to the surface of the sample is another method. This method has several disadvantages. Firstly, „overspraying“ under the edge of the mask. Secondly, shading part of the strip's workspace with the edge of the mask. These effects result in uneven edges, a reduction in the area of the mirror's working area, and partial dusting of nearby strips.

It is proposed in this paper to form „windows“ of the required size lithographically, and to spray them alternately into each „window“, which will eliminate the above-mentioned defects. The need to use lithography instead of classical masking is attributable to the complex shape of the strips and their small widths, on the order of hundreds of micrometers. It should also be noted that in practice, mirrors can be up to several hundred millimeters long. This paper describes a maskless direct-draw lithograph developed to address this problem that operates at 405 nm wavelength, which enables the sequential formation of strip mirrors on a single substrate. The lithograph has found a number of other applications in the course of its operation, which are also reported in this paper.

1. Technical device of the lithograph

A maskless direct writing lithograph (MDWL) is a device that combines the mechanisms of movement, exposure, and autofocus (Fig. 1) to form images on substrates coated with a photoresistive layer. The MDWL operation is based on the method of recording a partially absorbed laser beam reflected back from the sample surface, followed by recording it on a highly sensitive video camera. The recorded beam is processed by the control program, which then adjusts the position of the optical system node along the Z axis to focus on the sample surface. Thus, it is possible to control the focusing of the laser beam during exposure and movement of the sample, regardless of the topology of the sample surface.

The device consists of the following elements (Fig. 2):

1. Diode laser with fiber input and Fabry–Perot resonator (SLDP-405-10-SM) with an operating wavelength 405 ± 10 nm and a maximum power of 15 mW. Power control allows adjusting the intensity of the laser beam for obtaining the ability to work with different types of photoresist (depending on the type and methods of applying photoresist, the thickness of the resistance mask layer may vary).

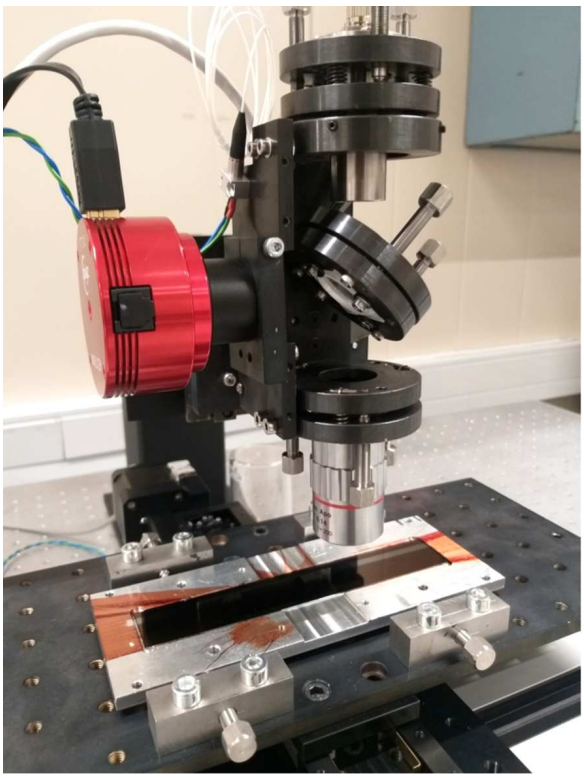

Figure 1. Photo of a maskless direct drawing lithograph. A silicon substrate with dimensions of 150 × 20 mm is installed on the desk.

2. Optical system consisting of:

a. Focusing lens with a diaphragm, which is used as a collimator to form a plane-parallel beam, with the ability to change the distance between the lens and the laser. An aperture with 4 mm hole, located directly after the focusing lens, is necessary for fixing the size of a plane-parallel beam calculated from the dimensions of the camera matrix.

b. Semi-transparent mirror in the form of a quartz cylinder with a thickness of 10 mm and parallel faces. The laser beam, passing through the diaphragm, hits the surface of the mirror, is refracted and partially reflected, then the refracted light is reflected from the sample back to the mirror, where it is again refracted and partially reflected. The partially reflected laser beam is captured and processed by a video camera.

c. Focusing lens with a numerical aperture of 0.055, working distance of 40 mm and depth of focus 91 μm. It is necessary for focusing a laser beam into a spot with a diameter of up to 10 μm, which is used for exposure and image formation in the photoresistive layer.

3. High-sensitivity high-speed video camera based on a monochrome CMOS matrix. Camera resolution 3096 × 2080, pixel size 2.4 μm, matrix size 7.4 × 5.0 mm. The maximum shooting speed is 60 fps.

4. High-precision system for moving along the XYZ axes using motorized linear translators. Linear translators for moving along the X and Y axes represent a perpendicular system in the form of a coordinate table. Full step resolution 2.5 μm with the ability to move the sample by 100 and 200 mm, respectively. The range of movement along these two axes can be increased by installing longer translators. The coarse and fine adjustment system is responsible for moving the optical system assembly along the Z axis, which is a long-stroke linear translator (40 mm) with a lock for coarse focusing, and a program-controlled mechanized linear translator with a 25 mm stroke for fine focusing of the laser beam, with full-step resolution 1.25 μm.

5. Each element of the MDWL is positioned and secured during alignment using a set of micro-screws.

Additional removable elements:

1. A set of removable diaphragms required to align the elements of the optical system with each other. The diameter of the hole in each diaphragm is on the order of 200 μm.

2. The lithograph is provided with a removable light filter to perform primary laser focusing on the surface of a sample with a photoresist applied. This filter limits the operating spectral range of the laser, leaving only a part of the visible light sufficient for recording on a video camera. This element allows abandoning the second laser, which is usually used as an alignment laser.

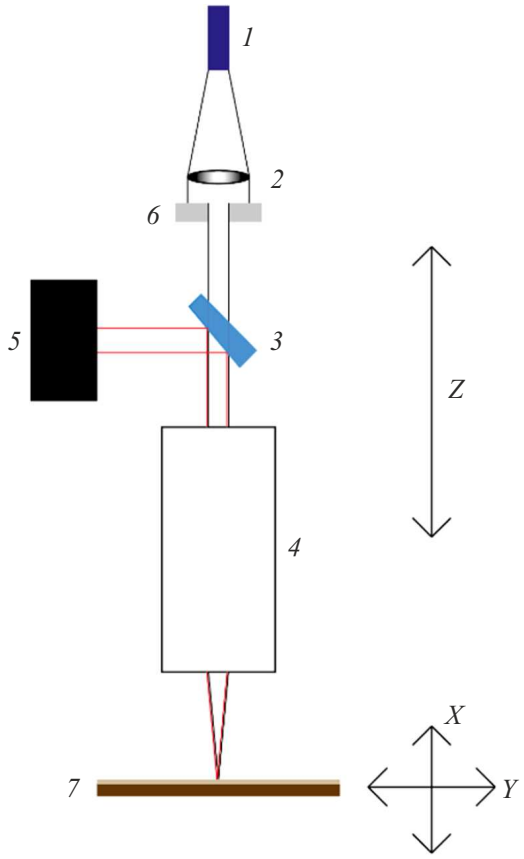

Figure 2. Block diagram of MDWL: *1* — diode laser; *2* — focusing lens; *3* — translucent mirror; *4* — focusing lens; *5* — high-sensitivity high-speed video camera; *6* — aperture Ø4 mm; *7* — substrate with applied photoresist.

2. Program part

The lithograph is controlled using software developed at IPM RAS. This program provides control capabilities both in manual mode (moving the linear translators by a given amount, turning on and off the laser, controlling the camera), and in the mode of executing commands from a file. Manual mode allows performing the initial preparation of the lithograph for operation, the mode of reading commands from a file allows highlighting complex shapes in the automatic mode.

The graphical interface is written in the Java programming language using the Swing library. Commands from the computer are transmitted to the central controller via a TCP socket. In this case, client–server communication is implemented, in which the computer acts as the client, and the central controller acts as the server. Further, commands from the central controller are transmitted to the peripheral controller, which directly interacts with the device (in this case, with the slides and the laser). The peripheral controller receives the message from the central controller, decodes it in accordance with the data exchange protocol, checks the checksum, and then executes the command. If the checksum check (data integrity check) or timeout check (limit time for the controller's response to a command) fails, the corresponding state is displayed in the GUI, and the command is not executed accordingly.

The linear translator are provided with stepper motors, which are controlled via drivers, the inputs of which are connected to the outputs of the controller. In order to shift the movement by a given distance, the controller output is supplied with synchro pulses with a given frequency, which determines the speed of movement (optionally configured). Synchro pulses are fed using timer interrupts, which allows guaranteeing the stability of steps over time. The duration of one clock pulse is $20\,\mu$s. The direction of movement of the linear translator is determined by the voltage at the corresponding output of the controller. A synchronous step along different axes is performed using a bit mask superimposed on the controller's system variable, which determines the potential value at the corresponding outputs. Libraries that configure the timer operation, as well as perform data exchange between controllers, are also developed at the IPM RAS. Each of the linear translators is provided with a limit switch connected to the controller input. When the end cap is closed (corresponding to the situation when the linear translator has run over the end cap), the movement stops, which allows preventing any damage to the linear translators. At the same time, the limit switches are provided with debouncing, which allows avoiding false positives. The laser is also controlled via a power supply unit with the ability to adjust the power.

One of the features of this lithograph is the autofocus mode, which allows maintaining the required size of the laser spot on the sample during photoresist illumination (Fig. 3). For operation in this mode it is first necessary to calibrate the height of the lens along the z axis (the vertical axis that determines the position of the lens above the sample, and therefore the illumination area). Calibration is performed as follows. The photoresist is illuminated at different points of the sample for a number of values of the z axis (the illumination points should not overlap). Next, the coordinate along the z axis corresponding to the smallest size of the highlighted area (focus) is selected. Then, a photo of the beam is taken using a camera connected directly to the computer. This frame determines the size of the beam on the camera, which corresponds to the laser focusing on the sample. The beam size on the camera is analyzed in the process of photoresist illumination in the operating mode. The axis z begins to shift until the beam size becomes equal to the reference size (Fig. 4) if the current beam size on the camera differs from the

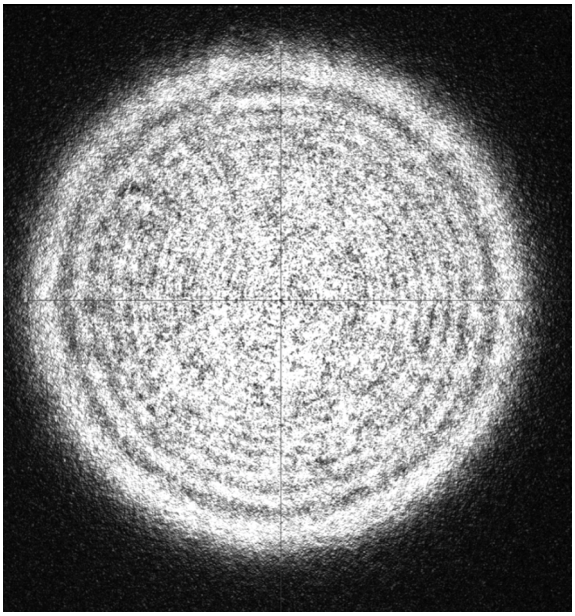

Figure 3. Image of the laser beam on the camera.

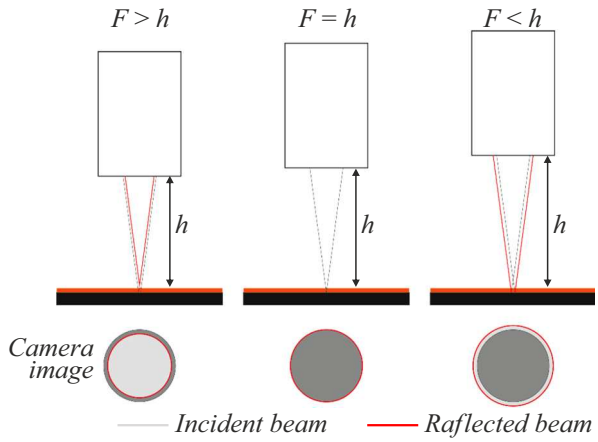

Figure 4. Principle of operation of the autofocus system. F — focal length, h — distance between the lens and the sample surface.

size corresponding to the beam focused on the illuminated sample. The usage of a special library to control the camera allows working with it from the same program that regulates the movement of linear translators and the operation of the laser.

The size of the beam on the camera is determined as follows. A command to shoot is sent to the camera via the USB port from the lithograph control program. Next, the camera status is polled in the loop to find out its current status. The data from the camera are written to a byte array (a two-dimensional matrix) as soon as the camera status indicates that the image is ready. The elements of this array correspond to pixels in the image, and the values recorded in the array cells correspond to the intensity of the corresponding pixel. Next, the beam center is determined. The average intensity is calculated for each row for this purpose (summing up all intensities of matrix cells by columns and dividing by the number of columns). After that, the element with the maximum average intensity is selected, which is considered the maximum coordinate along the Y axis (vertical). Similarly, the matrix element corresponding to the maximum on the horizontal axis X is determined by averaging the intensity for each column. As a result, the center of the beam is considered to be the point with the coordinates obtained above (x, y). The use of averaged intensities in determining the center avoids the impact of „bouncing“ intensity. Then, each axis is searched relative to the center for points where the averaged intensity decreases by a given number of times (this coefficient is chosen experimentally). The distance between these points is considered the beam size. At the same time, the autofocus algorithm checks the condition that the ratio of beam sizes along the horizontal and vertical axes should not be greater than 1.3 and less than 0.7, since this case corresponds to the fact that only a part of the beam is displayed on the camera, and then its size will be determined incorrectly. Therefore, the autofocus is turned off if this condition is violated and the user should adjust the optical circuit.

At the same time, the camera sends the next command to the image to speed up the program and avoid unnecessary time delays while the previous frame is being processed. Commands are also sent to the controller and data visualization is performed asynchronously.

The program opens the specified file in the automatic mode (reading commands from a file), and then starts executing commands to control the lithograph. The laser is switched on and off synchronously with the operation of the linear translator. The laser is turned off and the file is closed after execution of all commands. However, there is an option to run the same file again from the beginning. It is also possible to stop execution of commands, after which commands from the file can be executed starting from the first unprocessed command. Autofocus is also synchronized with the execution of commands from the file. In this case, the next command is not executed until the previous one is fully executed. This method allows highlighting random shapes, both with filling (highlighting of the inner area with a given step along one of the axes), and without it.

In addition to the autofocus function, this program provides the ability to highlight photoresist applied to surfaces whose shape differs from flat ones. In this case, the z axis is adjusted not by analyzing the beam image on the camera, but by setting the value of the coordinate of the z axis through a function that determines the surface shape. This method has already been tested on spherical surfaces.

This program is suitable for any linear translators provided with a stepper motor and performing linear movement. In the case of replacement of a linear translator, you should set the prescaler value (number of steps per μm) corresponding to the new shift, as well as select the optimal operating current of the stepper motor driver. However, this program can also be upgraded to control a large number of axes.

3. Method of manufacturing microstructures using MDWL

Commercial positive photoresist FP-051Ki from „Frast M“ was used for frabrication of microstructures. The photoresist was applied by centrifugation at 3000 revolutions per second. This was followed by pre-exposure heating in a drying cabinet with air blowing and at temperature of 85°C for 1 h. The thickness of the resistive mask layer under these conditions was about 2.5 μm.

The sample was fixed on the optical table of the MDWL after formation of the resistive mask. The workpiece was positioned using a set of micro screws. After autofocusing on a test mirror without a resistive mask to level out spurious illumination on the working sample, the control program was started with the specified parameters: the width and length of the exposed area, as well as the step of movement or the number of bands formed by the laser on 1 mm of the surface.

The exposed regions were developed after formation of an image on the photoresistive layer using MDWL at a laser beam power of 7 mW. The lithographic image was developed using standard commercial buffer developer based on UPF-1B alkaline solutions diluted with deionized water in the ratio of 1 : 4.5 by volume.

Then, a multilayer X-ray mirror was sputtered through the resulting resistive mask. Subsequent opening of the resistive layer by repeated washing in DMFA (N,N-dimethylformamide) allows removing the layer of a multilayer X-ray mirror located on the resistive layer, forming a microstructure, for example, a strip element with a given geometric shape. Cleaning in an oxygen plasma for 30 min was used for complete removal of organic residues of the resistive mask from the surface.

Multiple repetition of the processes described above makes it possible to form multi-strip multilayer X-ray mirrors. The block diagram of all stages is shown in Fig. 5.

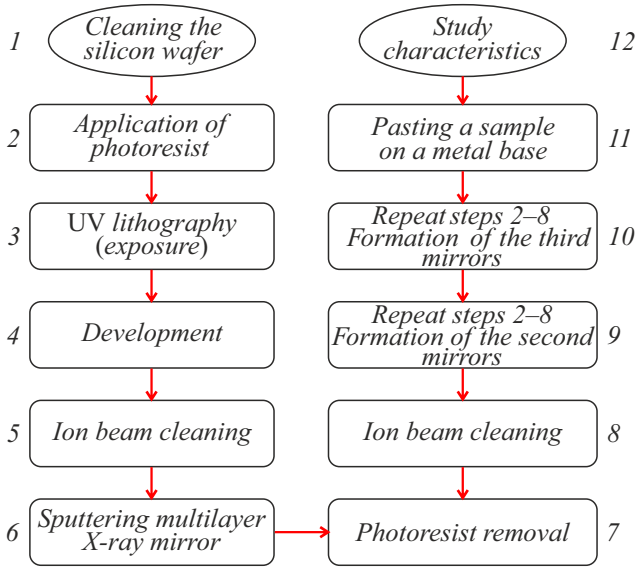

Figure 5. Technological process of formation of a multi-strip multilayer X-ray mirror. *1* - - - preparation of the silicon base; *2* — photoresist application; *3* — UV lithography (exposure); *4* — development; *5* — ion purification; *6* — sputtering of a multilayer X-ray mirror; *7* — opening (removal) of photoresist; *8* — ion purification; *9* — repeating items *2–8*, forming a second mirror; *10* — repeating items *2–8*, formation of a third mirror; *11* — pasting on a metal base; *12* — study of mirror characteristics.

Figure 6. Experimentally obtained multi-strip multilayer mirror for the two-mirror monochromator of SKIF synchrotron.

It should be noted that an important aspect in the fabrication of such mirrors is the adhesion of the sprayed multilayer X-ray mirror to the substrate surface, since partial or complete detachment of the sprayed layer can occur with multiple repetition of the strip formation processes. This problem can be solved by sputtering an additional metal sublayer that has better adhesion to the substrate and multilayer mirror materials.

4. Examples of completed work

Currently, the designed lithograph is intensively used in the development of multilayer X-ray optics and devices based on it. In particular, it was proposed to fabricate a strip mirror as part of the creation of a two-mirror monochromator of SKIF synchrotron with the monochromator operating energy range of 10–30 keV. This strip mirror is an assembly on a single substrate of thin (up to 4 mm wide) and long (up to 300 mm long) multilayer mirrors, which differ in the multilayer structure period. The following multilayer mirrors are used as strips in this paper: Mo/B_4C mirrors, ensuring high reflection coefficients and spectral selectivity at the level of 1. 5% in the photon energy range of $E \sim 10-20$ keV [6], W/B_4C mirrors, traditionally used in the energy range of above 20 keV [7,8], and Cr/Be mirrors, combining high reflection coefficients and spectral selectivity of $\Delta E/E \sim 0.3\%$ [9]. A photo of the experimental three-strip sample is shown in Fig. 6.

Another important application of the lithograph is the formation of microstructures on curved surfaces. An MDWL operation algorithm forming thin (about 200 μm) strips on the surface of the treated sphere was developed within the framework of the work for improving the accuracy of surface profile derivation for the procedure of symmetric (including aspherization of the surface shape) ion processing of curved substrates. The image is formed in such a way that the „step“ obtained during etching falls completely into the frame of the white light interferometer with the field of view of 0.9×0.9 mm. Thus, it was possible to eliminate the inaccuracy of determining the etching depth along the sample. The autofocusing is not performed during operation of the lithograph due to the unregistered (the percentage of reflected radiation is insufficient for the operation of the autofocus system) reverse reflection of the laser beam, as well as the inclination of the surface of the sphere. The primary focus adjustment of the laser beam is performed by placing a silicon plate on the edge of the sphere, followed by focusing on its surface and subtracting the thickness of the plate. Further, the movement of the node of the optical system is performed by the control program using a function based on the radius of curvature of the sphere used. An example of such a sample is shown in Fig. 7.

The authors are also working on the fabrication of experimental photomasks for contact lithography. Pho-

Figure 7. 200 μm strips formed on a concave spherical substrate.

tomasks are the most important tool of the lithographic process that allows forming the most complex topology of microelectronic devices on the resistance layer. In particular, photomasks can be used to produce free-hanging membranes Si_3N_4 [10]. The method of fabrication of such a template using the MDWL includes several main stages. First, the preparation of a borosilicate glass plate with a certain thickness, cleaning, and spraying on its surface a chrome layer with a thickness of about 200 nm. Next, a resistive mask is applied to the chrome layer. A mask representing a certain number of squares of a given size at a calculated distance from each other is formed on the photoresist using MDWL. The development of the exposed area of the resist allows the formation of „windows“ in the resistance mask, through which ion etching of the chrome layer is carried out at the next stage, forming a predetermined pattern directly on the metal layer. The final step in obtaining a finished photomask is to remove the remnants of the photoresist mask, first with the help of organic solvents, and then with the help of oxygen plasma treatment. The use of MDWL for fabrication of templates has great potential, as it significantly reduces the production process, which under normal conditions can take weeks and months; it allows creating structures of any shape and complexity, which, in turn, opens up wide prospects for solving a variety of technical problems.

Conclusion

A maskless direct-writing lithograph with the ability to automatically focus the laser beam on the sample surface was developed. Software was developed that controls all the nodes of the device. The developed device makes it possible to form „windows“ in a photoresistive layer with a beam diameter of 10 μm, with a displacement accuracy of up to 2.5 μm and an edge evenness of up to 10 μm. The obtained lithograph was successfully tested in the manufacture of multi-strip multilayer X-ray mirrors, and is used in methods for correcting the shape of high-precision curved substrates.

The lithograph design has the potential for modernization. In particular, the algorithm of the control program will be improved for increasing the speed and accuracy of the device's autofocus. For tasks requiring higher spatial resolution, the lithograph design provides for the replacement of the Mytutoya lens with a higher numerical aperture, up to $NA = 0.55$. As shown earlier, such a lens allows obtaining a resolution of up to 0.6 μm [11]. At the same time, there is no need to rearrange the device and replace the seat for the entire line of lenses of this type.

For work with spherical surfaces, it is possible to upgrade the axis displacement system XY with the replacement of the linear translator of one of the axes with a motorized rotary platform assembly with a motorized inclined platform. Such a design will allow the spherical surface to be tilted along the axis Z, thereby allowing the laser beam reflected from the sample to be directed back into the camera (in the current version, when working with curved surfaces, the laser is reflected to the side and is not registered by the camera), which in turn will allow the autofocus of the entire system to be maintained. The rotary platform will allow rotating the sample along its axis, forming a curved pattern. The upgrading of the control program by calculating the displacement of the recorded beam on the video camera matrix is also necessary for this version of the displacement system.

It is also planned to expand the functionality of the control program with such functions as automatic positioning of the laser beam relative to the illuminated sample, combining between successive iterations of strip mirror elements, determining the dimensions of the sample for virtual superimposition of the generated pattern on the sample, a system for reverse visualization of the MDWL operation process to track the percentage of completion of a running task. In particular, this will require the installation of an additional module for visual control of the alignment. In general, the planned improvements and upgrades of the lithograph developed by us will allow expanding the range of technical tasks solved by this device.

Funding

The development of the lithograph, the manufacture and testing of experimental samples were carried out with the financial support of the Russian Science Foundation grant No.21-72-30029. The lithograph was fabricated and assembled within the framework of the state assignment FFUF-2024-0022.

Conflict of interest

The authors declare that they have no conflict of interest.

References

[1] S.S. Morozov, S.A. Garakhin, N.I. Chkhalo. J. Surf. Investigation: X-ray, Synchrotron Neutron Techniques, **17** (1), S250 (2023). DOI: 10.1134/S1027451023070340

[2] N.I. Chkhalo, S.A. Garakhin, I.V. Malyshev, V.N. Polkovnikov, M.N. Toropov, N.N. Salashchenko, B.A. Ulasevich, Ya.V. Rakshun, V.A. Chernov, I.P. Dolbnya, S.V. Raschenko. Tech. Phys., **92** (8), 1261 (2022) (in Russian). DOI: 10.61011/TP.2024.08.59007.165-24

[3] S.S. Morozov, G.D. Antysheva, N.I. Chkhalo. Materialy simpoziuma „*Nanofizika i nanoelektronika — 2024*“ (Nizhnij Novgorod IPF RAN, Rossiya, 2024), t. 1, s. 492 (in Russian).

[4] M. Schuster, H. Gobel. J. Phys. D: Appl. Phys., **28** (4A), A270 (1995).

[5] M.M. Barysheva, I.V. Malyshev, V.N. Polkovnikov, N.N. Salashchenko, M.V. Svechnikov, N.I. Chkhalo. Kvantovaya elektronika, **50** (4), 401 (2020) (in Russian).

[6] R. Shaposhnikov, V. Polkovnikov, S. Garakhin, Y. Vainer, N. Chkhalo, R. Smertin, K. Durov, E. Glushkov, S. Yakunin, M. Borisov. J. Synchrotron Rad., **31**, 268 (2024).

[7] C. Morawe, R. Barrett, K. Friedrich, R. Klünder, A. Vivo. J. Phys. Conf. Ser., **425**, 052027 (2013).

[8] P.C. Pradhan, A. Majhi, M. Nayak. J. Appl. Phys., **123**, 095302 (2018). DOI.org/10.1063/1.5018266

[9] R. Pleshkov, N. Chkhalo, V. Polkovnikov, M. Svechnikov, M. Zorina. J. Appl. Crystal., **54** (6), 1747 (2021). DOI.org/10.1107/S160057672101027X

[10] D.G. Reunov, N.S. Gusev, M.S. Mihajlenko, D.V. Petrova, I.V. Malyshev, N.I. Chkhalo, ZhTF, **93** (13), 1032 (2023) (in Russian). DOI: 10.61011/TP.2024.08.59007.165-24

[12] N.I. Chkhalo, A.E. Pestov, N.N. Salashchenko, A.V. Sherbakov, E.V. Skorokhodov, M.V. Svechnikov. Rev. Sci. Instrum., **86**, 063701 (2015). DOI.org/10.1063/1.4921849

Translated by A.Akhtyamov